



LAWRENCE  
LIVERMORE  
NATIONAL  
LABORATORY

# Ceramic Laser Materials

T. F. Soules, B. J. Clapsaddle, R. L. Landingham,  
K. I. Schaffers

February 16, 2005

## Disclaimer

---

This document was prepared as an account of work sponsored by an agency of the United States Government. Neither the United States Government nor the University of California nor any of their employees, makes any warranty, express or implied, or assumes any legal liability or responsibility for the accuracy, completeness, or usefulness of any information, apparatus, product, or process disclosed, or represents that its use would not infringe privately owned rights. Reference herein to any specific commercial product, process, or service by trade name, trademark, manufacturer, or otherwise, does not necessarily constitute or imply its endorsement, recommendation, or favoring by the United States Government or the University of California. The views and opinions of authors expressed herein do not necessarily state or reflect those of the United States Government or the University of California, and shall not be used for advertising or product endorsement purposes.

This work was performed under the auspices of the U.S. Department of Energy by University of California, Lawrence Livermore National Laboratory under Contract W-7405-Eng-48.



**FY04 LDRD Final Report**  
**Ceramic Laser Materials**  
**LDRD Project Tracking Code: 04-FS-006**  
**Thomas F. Soules, Principal Investigator**  
**Brady J. Clapsaddle, Co-Investigator**  
**Richard L. Landingham, Co-Investigator**  
**Kathleen I. Schaffers, Co-Investigator**

**Abstract**

Transparent ceramic materials have several major advantages over single crystals in laser applications, not the least of which is the ability to make large aperture parts in a robust manufacturing process. After more than a decade of working on making transparent YAG:Nd, Japanese workers have recently succeeded in demonstrating samples that performed as laser gain media as well as their single crystal counterparts. Since then several laser materials have been made and evaluated. For these reasons, developing ceramic laser materials is the most exciting and futuristic materials topic in today's major solid-state laser conferences.

We have established a good working relationship with Konoshima Ltd., the Japanese producer of the best ceramic laser materials, and have procured and evaluated slabs designed by us for use in our high-powered SSHCL. Our measurements indicate that these materials will work in the SSHCL, and we have nearly completed retrofitting the SSHCL with four of the largest transparent ceramic YAG:Nd slabs in existence.

We have also begun our own effort to make this material and have produced samples with various degrees of transparency/translucency. We are in the process of carrying out an extensive design-of-experiments to establish the significant process variables for making transparent YAG.

Finally because transparent ceramics afford much greater flexibility in the design of lasers, we have been exploring the potential for much larger apertures, new materials, for example for the Mercury laser, other designs for SSHL, such as, edge pumping designs, slabs with built in ASE suppression, etc. This work has just beginning.

**I. Introduction/Background**

**A. What are transparent ceramics?**

Ceramic materials are formed by first taking powders of a refractory material, for example, an oxide, fluoride, etc. and then cold pressing the powder or adding a suitable binder and extruding the slurry, slip casting it or otherwise forming the slurry into a desired shape and then burning off the binder. The powder will maintain the compact form, known as the green structure, the grains being held together by van-der-Waals forces. Typically the green structure has a density 50-60% of the theoretical density, that is, the density of the bulk material.

The green structure is then heated to 80-90 % of its melting temperature to start the sintering. Sintering begins with neck growth between particles. Neck growth is driven by a reduction in surface energy. Solid-vapor surface energy is replaced with solid-solid intergranular surface energy by the migration of surface atoms to the region where particles are in contact. In this stage of the sintering there is little change in density. Because neck growth is driven by reduction in surface tension energy, sintering is facilitated using a large surface area to weight ratio powder. Nano-sized particles sinter much more easily than micrometer sized particles.

In the next stage the void volumes between particles become rounded and cylindrical and shrink in size. The grains resemble fused tetrakaidecahedra with tubular void regions along edges. The vacancy tubes shrink in diameter and the density of the structure goes up from to  $\sim 93$  % of the theoretical density.

Ultimately the open tubular porosity breaks up into spherical pores due to surface tension. The small isolated pores are at vertices of the tetrakaidecahedra. This closed porosity is difficult to remove and must be removed by vacancy migration along grain boundaries. Increasing the temperature also promotes grain boundary migration. Grain boundaries can break free of the pores and trap them within the grains themselves making them even more difficult to remove since they now can be removed only by vacancy migration through the grain.

## **B. Brief History of transparent ceramics**

R. Coble (US Patent No. 3 026 210, 1957; J. Appl. Phys. 32, 793, 1961) while he was at the General Electric Company Corporate Research Center solved this problem while sintering alumina powder by adding approximately 2 % magnesia. The magnesia acted as a grain growth inhibitor and Coble<sup>2</sup> invented Lucalox<sup>TM</sup>. Lucalox is translucent, meaning that it transmits light diffusely. It is not transparent. Lucalox fabricated in tubular form is used as the arc chamber to contain high pressure sodium discharges used in all yellowish street lamps.

This author (GE Internal report, 1972) and Peelan (Philips Tech. Rev. 36, 47, 1976) modeled light transmission through a Lucalox plate using Monte-Carlo ray tracing methods. Light rays striking randomly oriented grain boundaries followed either the reflected or refracted ray based on Fresnel equations and when they struck a pore, assumed to be spherical, there scattered direction was chosen using Mie scattering intensity distributions. The bottom line of this investigation was that pores not grain boundaries were mainly responsible for the light transmission characteristics of Lucalox and that if one wanted to make transparent polycrystalline alumina one needed to go reduce porosity to  $10^{-5}$  to  $10^{-6}$ .

C. Greskovich and Chernoch (J. Appl. Phys. 44, 4599, 1973) made the first laser using a transparent ceramic, yttria doped with neodymium and using thoria as the grain growth inhibitor. More recently the General Electric Company and Siemens have developed yttrium gadolinium oxide doped with europium and gadolinium oxysulfide doped with praseodymium as transparent ceramics for scintillation counters used in their computer aided tomography (CAT) scan X-ray units. The scintillation counters while they are transparent are not of laser quality.

The real interest in transparent ceramics for lasers was sparked in the late 1990's when two groups in Japan, one lead by A. Ikesue, et al. (J. Amer. Ceram. Soc.

78,1033,1995) using a solid-state reaction method for making YAG powder and the other lead by the Konoshima Chemical Company and T. Yanagatani (Jap Patent No. 10-101411) using nanoparticle co-precipitates succeeded in making transparent YAG:Nd by sintering in a vacuum furnace and demonstrated laser performance equal to or superior to single crystal YAG:Nd lasers.

### C. Requirements for a ceramic to be transparent

The scanning electron microscope (SEM) picture in Figure 1(A) shows the grain structure of a transparent YAG sample. Grains range from 1-~5 micrometers in diameter, and there are no pores in the picture. Pores would appear as small filled black circles. Also the grain shapes do not necessarily resemble cross sections of tetrakaidecahedra but in some cases the grain boundaries look like fused crystal cleavage planes as is also indicated by the transmission electron micrograph (TEM) in Figure 1 (B). A. Searcy (<http://www.lbl.gov/Science-Articles/Archive/ceramic-sinter.html>) argues that while no doubt surface energy is minimized during grain growth the simple model based on spherical particles is probably not correct and the energetics of crystal facets must be considered. In particular he points out that LiF sinters without first spherodizing.

The TEM also shows that the grain boundary width is only  $\sim 1$  nm, much less than the wavelength of the IR radiation at  $\sim 1064$  nm. Hence vertices formed by the confluence of grain shapes would not be expected to scatter this light.

Hence the conditions for having a transparent ceramic are: (1) essentially no porosity. The total pore volume being  $< 10^{-5}$  to  $10^{-6}$  as mentioned above. Also since the grain facet lengths are on the order of the size of the wavelength of light, so that there will be no reflection or refraction of light, the refractive index on both sides of grain boundaries should be equal, that is, cubic crystals with no birefringence. Also to avoid any reflection or refraction at grain boundaries the powder must be very phase pure.

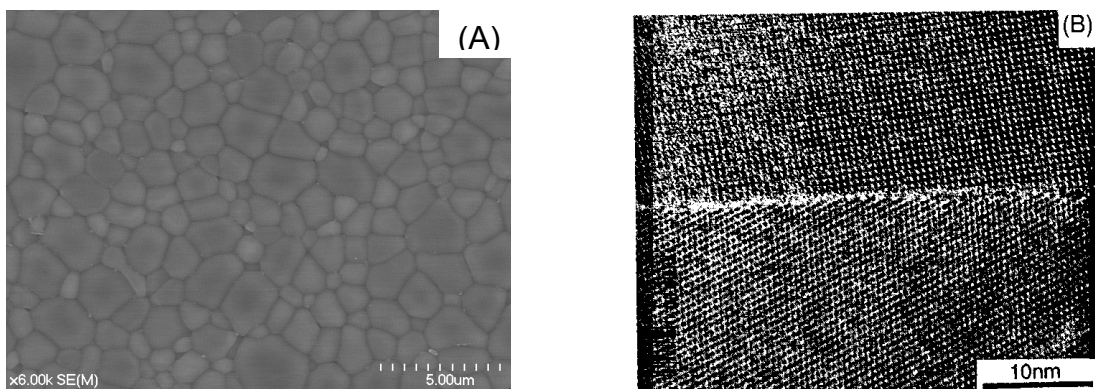


Figure 1. 1(A) is a scanning electron micrograph (SEM) of an etched sample of transparent YAG produced by Konoshima Ltd. 1(B) is a transmission electron micrograph (TEM) showing a grain boundary in the same sample.

#### **D. Advantages of transparent ceramics for laser applications**

Although producing transparent ceramics is difficult with many process steps which must be carefully controlled, the advantages, not the least of which is the fact that once the process is developed and put under control samples can be made reproducibly with relatively high yields, make ceramics a very attractive alternative to single crystals. Lucalox arc tubes and ceramic scintillation counters are made in large quantities with high yields. On the other hand, the making of large single crystal boules particularly of highly refractory materials is still an art with yields often going from 100 % to 0 % and anywhere between at any time for unidentified causes.

Other advantages of ceramics for laser applications include being able to dope ceramics to much higher levels than single crystals. High dopant levels in single crystals can lead to cracking. Also in ceramics the dopants are uniformly distributed while in single crystals they tend to be more heavily concentrated near the bottom of the boule due to zone refining. Also the concentration in the melt is generally much higher than that in the crystal so that a segregation coefficient must be used to calculate the dopant concentration in the crystal from that in the initial formulation.

Growing single crystals by Czochralski pulling of a seed crystal from the melt in a thermal gradient results in a residual stresses. There is typically a highly stressed core with the stress pattern radiating outward. This may lead to depolarization effects or in the worst case may lead to the crystal cracking either when cooling or during operation.

Finally ceramics are in general tougher than single crystals. Hardness as measured by  $K_{1C}$  for ceramic YAG is more than 3 times that of the single crystal. The reason for this is that cracks which radiate out from, for example, an indenter impressed on the single crystal are blunted by grain boundaries in the case of the ceramic.

Ceramics also offer the possibility enhancements to laser performance that are not possible with single crystals. For example apertures are scalable providing a potentially scalable laser power. Ceramics can be made as large as the hot zone of the vacuum furnace and apertures >20 cm are possible. On the other hand the difficulty in growing single crystals goes up exponentially with increasing boule diameter and in the case of Czochralski growth it may ultimately be limited by the weight of the crystal boule.

Ceramics can be formed in different shapes, for example, Lucalox arc tubes made by extruding the slurry and binder. Slip casting allows almost any open shell shape. Different shapes could provide improved pump light coupling and heat transfer during lasing. Multiple functionalities in a single monolithic piece are also possible with ceramics and one can even imagine tailoring the ceramic on a mesoscopic scale, that is, the scale of the grain size. Our efforts to capitalize on the flexibility of ceramics in laser designs is just beginning but some ideas are mentioned near the end of this report.

#### **Research Activities**

Our research activities were aimed at three objectives. First we planned to procure and evaluate transparent ceramic YAG:Nd for use in the solid-state heat capacity

laser (SSHCL). Our second objective was to learn as much as possible about the synthesis of transparent ceramic YAG for the purposes of being an informed consumer and possibly providing a second domestic source of this new material. Our third objective was to help optimize the overall laser design for using ceramic laser materials including obtaining some intellectual property in doing so.

#### **A) Evaluation of Konoshima/Baikowski ceramic YAG:Nd**

First we reviewed the literature including the Japanese patent literature and visited Synoptics Northrop Grumman and VLOC a division of II-IV Incorporated and reviewed their ceramic YAG efforts. Two small (<1 cm in width and a couple millimeters in thickness) sized pieces of transparent YAG:Nd were obtained from VLOC for our measurements. Some measurements were made and discussed below and the samples returned to VLOC. VLOC had an agreement with Professor Gary Messing of Penn State to work on developing a synthesis for ceramic YAG and this was funded from the JTO.

However, we decided our best chance of obtaining transparent ceramics in the near future of the size and quality needed for the SSHCL were to directly contact Konoshima, Ltd. in Japan. Konoshima Ltd. was the only company producing these ceramic materials commercially and selling them to laser manufacturers. Konoshima was contacted through Justin Otto of Baikowski International. Baikowski works directly with Konoshima and Baikowski, Japan polishes the Konoshima ceramics for laser applications.

We challenged Konoshima to make a laser quality slab of YAG with 0.3 at % Nd 10x10x2 cm in size which could be retrofit directly in the laser. We also provided other specifications with regard to surface flatness, ripple, inclusions and dislocations. These numbers are on the SSHCL engineering drawings. Konoshima replied that they could not make a slab of this thickness but could produce a slab

10x10x0.6 cm and meet our other specifications. The concentration of Nd was chosen to be 0.8 at % to absorb the radiation from the pump diodes in the thickness available. This slab was ordered in mid May, 2004 for delivery in mid June. A picture of the slab which was received on time is shown in Figure 2 together with an epoxied blackened copper edge cladding which was designed for it to absorb amplified spontaneous emission (ASE).

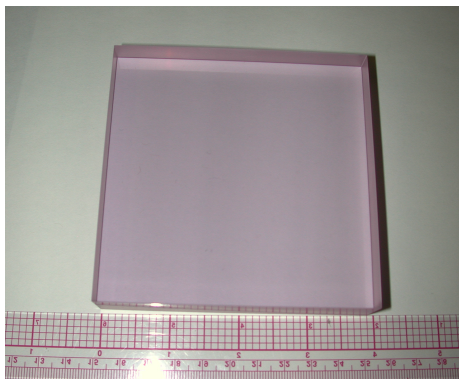


Figure 2. The 10x10x0.6 cm ceramic YAG sample with 0.8 at % Nd provided by Konoshima, Ltd. The figure on the right also shows the epoxied blackened copper edge frame designed to absorb ASE.

On May 17, 2004 we met with representatives of Konoshima including the inventor of the Konoshima ceramic YAG process, Dr. T. Yanagitani, as well as, the president and vice-president of Baikowski, Japan and Baikowski, International. We held an all day meeting. Technical tidbits regarding the Konoshima process, as well as, characteristics of the material, that were mentioned at that meeting, are reported in the Interim Report – June 8, 2004 for the Feasibility Study 04-FS-006.

Because the thin YAG:Nd sample with 0.8 at % Nd even when used together with our ASE absorbing frame clamped or underwent parasitic lasing almost immediately when used at full aperture with a YAG:Nd probe laser and our high power diode pump arrays, it was possible to make gain measurements only with a much smaller  $\sim 1$  inch aperture. Since this would not be acceptable in the high power laser application, we requested that Konoshima develop a process for making a 2 cm thick slab 10 x 10 cm YAG with 0.3 at % Nd. Dr. T. Yanagitani offered that this might be possible by partially sintering 2 thinner slabs and then sintering the two together. This development was undertaken and Konoshima estimated that a finished and polished slab would be available at the end of December, 2004. We agreed that if this slab was demonstrated to work in the SSHCL we would order four subsequent slabs at agreed upon pricing well below the commercial price Konoshima would market the slabs to industrial customers. In the middle of December, Baikowski delivered two 10x10x2 cm slabs of ceramic YAG:0.3 at % Nd. A second slab was provided with the first one because it did not meet our specification with regard to inclusions. It had  $\sim 10$  small inclusions which were carefully mapped by Baikowski. Figure 3 shows a picture of these two slabs along with one of the slabs, the one without the inclusions, epoxied into a blackened copper holder we designed for it. The holder was designed to support the slab in the SSHCL and was blackened to absorb ASE and was also provided with cooling channels that could be used to further cool the copper and epoxy or to control edge temperatures in order to improve wavefront control during heating in operation.

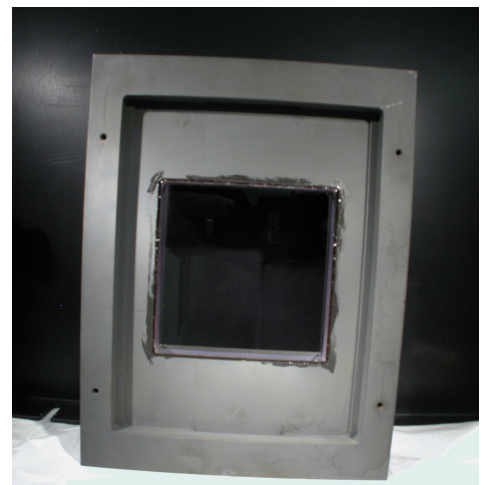


Figure 3. Two 10x10x2 cm transparent ceramic YAG amplifier slabs with 0.3 at % Nd provided by Konoshima, Ltd. in December, 2004. The figure on the right shows one of the slabs epoxied into blackened copper holder designed to absorb ASE and provide temperature control to the holder.

## **B) Development of an LLNL process for making transparent YAG**

### **1) Powders used**

Our first sintering experiments were made using YAG powder (99.99 % pure from MTI corporation in Richmond, California) with 70 nm median particle size.

Fine YAG powder was also obtained from Shin-Etsu (Lot # RYAG-OCX-074) through Pred Materials International, Inc. This material had a median particle size of 1.08 micrometers as measured on a Microtrac and came with a C of A which showed not detectable CaO, SiO<sub>2</sub> or Fe<sub>2</sub>O<sub>3</sub> and a loss on ignition of 0.15 %.

Nanoparticulate YAG powder was made at LLNL in CMS by three different routes. Because of the expertise at CMS in sol gel chemistry, the first samples were made using a sol gel method. The sol gel synthesis of YAG is described in detail in the Interim Report. Several batches of this powder were made.

Because the nanoparticles of YAG produced by the sol-gel route were highly agglomerated, we also made powder using an aerogel route. Water in the gelatinous sol is replaced with alcohol and heated in an autoclave to supercritical temperatures at which the surface tension is near zero and then allowed to escape. The aerogel is broken up and then calcined. The detailed experimental procedure is given below:

1. AlCl<sub>3</sub>·6H<sub>2</sub>O (14.02 g; 0.058 mol) and YCl<sub>3</sub>·6H<sub>2</sub>O (10.59 g; 0.035 mol) were dissolved while stirring in 150 g of 200-proof ethanol in a plastic container.
2. Following dissolution of the metal salt, 55 g of propylene oxide (PO) were added to induce gelation of the solution. (**CAUTION:** addition of PO to metal salt solutions may be accompanied by significant heat generation, which in some cases leads to flash boiling of the synthesis solution.)
3. After the addition of the epoxide, the solution was briefly stirred to ensure thorough mixing and the stir bar was then quickly removed. The reaction mixture was then covered and gelled to a solid monolith in about 2 minutes. The resulting gel remained covered and was aged for at least 24 h after the initial gelation.
4. Following aging, the gel was subjected to a pore-washing/solvent exchange step in 200-proof ethanol for 3–5 d. During this time, the wash solution was replaced at least three times with fresh ethanol.
5. Following pore washing, the wet-gel was processed to an aerogel using supercritical extraction techniques in a Polaron™ supercritical point dryer. After placing the wet-gel in the Polaron™, the ethanol in the wet-gel pores was exchanged for CO<sub>2</sub> for 3–4 days at ~12 °C and a pressure of ~55 bar.
6. Following complete solvent exchange, the temperature of the vessel was ramped to ~45 °C while maintaining a pressure of ~100 bar to obtain supercritical CO<sub>2</sub>.
7. The vessel was then depressurized at a rate of about 7 bar/h while maintaining a temperature of ~45 °C.

8. The resulting monolithic aerogel was gently ground to an extremely fine powder using a plastic spatula. The powder was then heat treated in alumina crucibles at 1000 °C (5 °C/min. ramp rate) for 2 hours in order to induce YAG crystallization.

Figure 4 shows a TEM of the resulting powder indicating generally spherical primary particles with a median particle size of  $\sim 10$  nm with still some agglomeration. Some of the samples were calcined at 475 C for  $\frac{1}{2}$  hour and others at 1000 C for  $\frac{1}{2}$  hr. The X-ray diffraction results show that heating to 475 C does not result in crystallization while calcining at 1000 results in complete conversion to YAG with a small amount of Y<sub>2</sub>O<sub>3</sub>. In subsequent work we have moved the calcining temperature to 1100 C to insure complete conversion and added a washing step with nitric acid to remove any Y<sub>2</sub>O<sub>3</sub>.

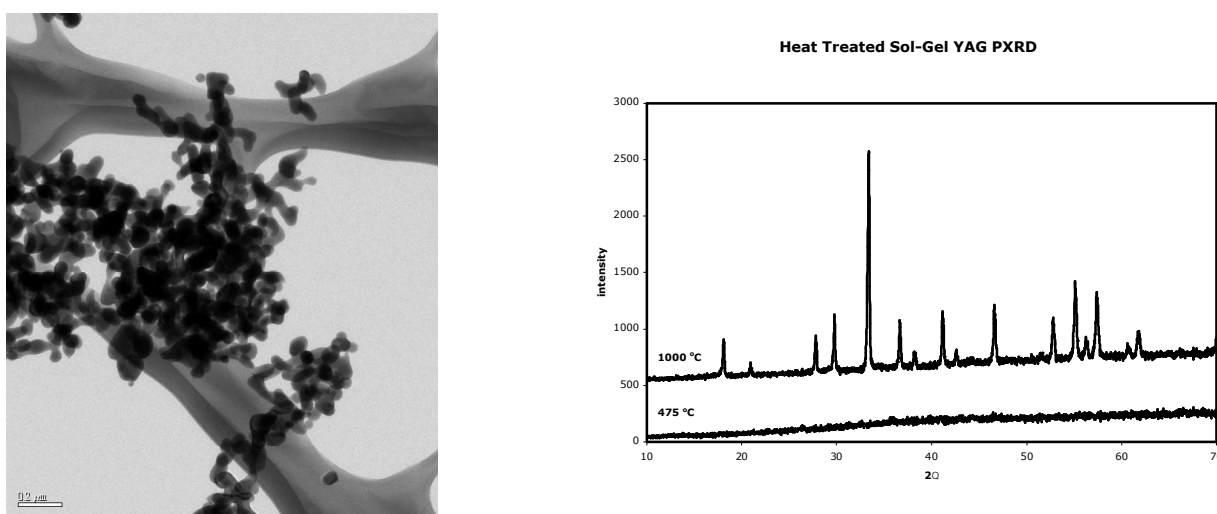


Figure 4. TEM of YAG powder synthesized using the aerogel route by Brady Clapsaddle and calcined at 1000C for  $\frac{1}{2}$  hr, and on the left the powder x-ray diffraction pattern.

Finally, we are also making nanoparticle YAG powder following precipitation methods similar to those documented in the Japanese patents (T. Kokai Patent App. # HEI 10[1998]-101333) and literature (Ji-Guang Li, T. Ikegami, J. Lee and T. Mori, J. Am. Ceram. Soc. 83, 961 (2000)) using ammonium hydrogen carbonate to co-precipitate aluminum and yttrium ions in solution. The details of this precipitation are given below:

1. Alum ( $\text{Al}(\text{NH}_4)(\text{SO}_4)_2 \cdot 12\text{H}_2\text{O}$ ; Fluka,  $\geq 99.0\%$ ), aluminum nitrate nonahydrate ( $\text{Al}(\text{NO}_3)_3 \cdot 9\text{H}_2\text{O}$ ; Alfa Aesar, 98.0 – 102.0%), yttria ( $\text{Y}_2\text{O}_3$ ; Alfa Aesar, 99.999%), and ammonium bicarbonate ( $\text{NH}_4\text{HCO}_3$ ; Alfa Aesar, 99%) were all used as received. Nitric acid ( $\text{HNO}_3$ ; J. T. Baker, 69.0 – 70.0%) was diluted with water in a 1:5 (v:v) ratio. All solutions were made using distilled, deionized water ( $\text{d}^2\text{-H}_2\text{O}$ ) with an initial resistivity of 18 M $\Omega$ .
2. Two separate 15 L solutions of 0.15 M  $\text{Al}^{3+}$ /0.090 M  $\text{Y}^{3+}$  were prepared with yttria (151.29 g, 0.67 mols) and either alum (1020.00g, 2.25 mols) or



aluminum nitrate nonahydrate (844.05 g, 2.25 mols) to obtain stock solutions containing  $\text{Al}^{3+}$  and  $\text{Y}^{3+}$  in a Al:Y molar ratio of 5:3.

3. The stock solutions were prepared by first slurrying the yttria and aluminum salt in 2.25 L of  $\text{d}_2\text{-H}_2\text{O}$  followed by addition of 0.6 L of the diluted nitric acid solution.
4. This mixture was then gently heated to  $\sim 80^\circ\text{C}$  until all solids were observed to be dissolved. After the mixture cooled to room temperature, the resulting solution was diluted to a final volume of 15 L.
5. Ammonium bicarbonate (2371.80 g; 30 mol) solutions were made at a concentration of 1.5 M in 20 L batches by dissolving the salt in  $\text{d}_2\text{-H}_2\text{O}$ . All stock solutions were stored at room temperature in 20 L, HDPE carboys prior to use.
6. For precipitation experiments, 1200 mL of stock metal salt solution (0.15 M  $\text{Al}^{3+}$ /0.090 M  $\text{Y}^{3+}$ ) was added drop wise to 1800 mL of stock  $\text{NH}_4\text{HCO}_3$  (1.5 M) containing a dispersant\* (0.15-0.5 mg/ $\text{m}^2$  Dispex™ (A40 40 wt % acrylic). During addition, the mixture was stirred\* (vigorous or gentle agitation) at the desired temperature\* (R.T. or  $90^\circ\text{C}$ ).
7. Following precipitation, the precipitate was aged (0 or 2 days) at room temperature without stirring.
8. The aged precipitate was then vacuum filtered, washed 4 times with  $\text{d}_2\text{-H}_2\text{O}$ , rinsed with ethanol, and dried at room temperature under flowing nitrogen.
9. The resulting cake was then ground with a mortar and pestle.
10. The ground powder was then calcined in air at  $1100^\circ\text{C}$  for 1 hour with a heating rate of  $2.5^\circ\text{C}/\text{min}$ .
11. Following calcination, some batches of powder were washed with 2 M  $\text{HNO}_3$ , followed by 4 washings with  $\text{d}_2\text{-H}_2\text{O}$ . Washed powders were dried at  $80^\circ\text{C}$  overnight.

The precipitated samples with the different conditions mentioned above are to be used in a design-of-experiments that will be described in the 2004 LDRD report.

## **2) Sintering methods**

Because LLNL did not have high temperature vacuum sintering capabilities, our first samples have been toll fired at outside facilities. A Thermal Technology vacuum furnace has since been acquired by CMS and will be operational shortly making it possible to not only make the powders but do the firing in-house.

### **Thermal Technologies**

The first sintering experiments were performed using the MTI powder. The powder was made into 1 inch diameter pellets by dry pressing and using a water slurry with and without a small 1 & 2 % silica as a sintering aid and with/without a Carbowax binder to improve dispersion in the slurry and was fired in a vacuum furnace ( $10^{-5}$  -  $10^{-6}$  torr) at Thermal Technologies in Santa Rosa, California for 12 hours at 1650, 1750 and 1850 C. Details are given in the Interim Report.

### **UC Davis**

Samples were also fired at the University of California at Davis using a Spark Plasma Sintering (SPS) hot press. The hot press uses graphite dyes and when the temperature reaches a preset value a current is passed through the sample to aid sintering and allow sintering at lower temperatures to excessive or abnormal grain

growth. The samples were ball milled for 12 hours and pressed into pellets before sintering. Dr. Umberto in Professor Zuhar Munir's group sintered the samples in the SPS. Sintering temperature ramps, final temperatures and current profiles can be obtained from Professor Munir. Because the graphite dies were used a reducing atmosphere is present which turned the samples dark gray or black in color. Afterward we fired the samples in air at 1550 C for 12 hours. This removed the black color and the resulting samples were white and translucent.

### **Greenleaf Corporation**

Samples were also hot pressed and hot-isostatic pressed (HIP'ed) and hot pressed following by HIP'ing at Greenleaf Corporation in Pennsylvania. Hot pressing was done at 4.5 ksi and 1750 and 1780 C and HIP'ing at 20.5 ksi and 1720 C. These samples were also dark gray in color due to graphite dies and had to be re-fired in air at 1550 C at which point they became white but essentially opaque.

### **Stanford University**

Because we do not have a vacuum furnace here at LLNL and had to have sintering experiments done at toll vendors (a vacuum furnace has been purchased by CMS and is installed but not yet completely hooked up) and because Dr. Romain Gaume under Professor Robert Byer at Stanford was also working on producing transparent ceramic laser materials, we joined with them to both sinter powders we made and plan experiments. The ceramics are sintered in a high temperature 5kW vacuum furnace made at Stanford. The heating element consists of a tungsten mesh assembly that provides a 3"x 3" hot zone surrounding a tungsten plate where the ceramic sample sits. Vacuum is achieved with a mechanical pump followed by a diffusion pump. A liquid nitrogen cold trap is used to prevent oil back streaming. The temperature is monitored by a remote type C thermocouple (W-Re 5%/ W-Re 26%), and a calibrated optical pyrometer (Minolta, Cyclops 512A). The pyrometer looks directly at the surface of the sample through a sapphire view port. The current running through the heater is also monitor. This system can reach 1850 °C under a vacuum of  $10^{-5}$  torr.



Figure 5. The vacuum furnace at Stanford University.

The sintering step follows a short soaking at 750°C for half an hour. This helps bake out any residual gases. The pressure is monitored during this soak and throughout the run with a cold cathode gauge and typically goes from  $10^{-4}$  torr at the beginning of the high temperature dwell to below  $3 \cdot 10^{-5}$  torr after 30 minutes at this temperature. The cycle ends by cooling the furnace at a rate of 600°C/h.

### **C) Other laser architectures using transparent ceramics**

A LLNL patent (IL-11317) was applied for covering roughening the edge of the gain media and using a high index epoxy to bond the ASE suppressor to the gain media slab. This patent application also covers the use of a blackened copper frame and a moat of this epoxy between the frame and the gain media slab as shown in the right hand side of Figures 2 and 3. Details of this work are described in a memo report dated September 17 and sent to legal. A copy of this report is attached.

Discussions were held at LLNL on January 28, 2005 with members of the SSHCL and later representatives from CMS and the Mercury program and with:

- Dr. Takagimi Yanagitani - Ceramic YAG Inventor and Manager,
- Mr. Takashi Shigeta - Baikowski Japan President,
- Mr. Shinichi Yuminami - Baikowski Japan YAG Sales Manager,
- Mr. Justin Otto - Ceramic YAG North American Sales Manager,
- Mr. Thomas Carbone - Baikowski International Vice-President.

We discussed some future design considerations, first for the SSHCL. These included making larger slabs perhaps 20x20x2 cm for still higher power lasers. The only issue expressed by Konoshima was the need for a larger furnace. Currently slabs can be made only up to 12 cm wide in the Konoshima furnace.

Also discussed was the possibility of monolithically including Sm doped YAG edge cladding. A 10x10x2 cm slab would be co-sintered with Sm doped edge cladding pieces. Konoshima said that this was possible and was being investigated. The process would be developed without any LLNL contract.

Konoshima has also provided us with ceramic YAG samples containing 3 and 5 at %  $\text{Sm}^{3+}$ . These were measured in the infrared on a Perkin-Elmer spectrometer. In addition to having the ASE suppression built-in, the use of YAG:Sm has the advantage that the laser diode pump light is not absorbed by Sm and therefore the method of pumping can be through the ASE suppressor, eg edge-pumping.

We also discussed the possibility of making a round or circular or hexagonal or octagonal slabs, again possibly with YAG:Sm<sup>3+</sup> edge cladding sintered directly. An approximately circular beam pattern has advantages in the design of the output coupler. Dr. Yanagitani said that it would be easier to co-sinter the edge cladding if the shape was approximately circular rather than square as the circular ring would naturally contract onto the slab with sintering with this geometry.

Other designs including composite designs were discussed briefly including the possibility of designs in which the diode pump light could be light piped to the gain media in a composite monolithic piece. We have several ideas for composite novel

laser ceramics with multiple functionalities built in a single piece. Other ideas remain proprietary. We have not prioritized these or started any serious design work much less experimental work on them. It is planned that this activity will pick up in FY 2005.

We also briefly discussed other materials that could be sintered into transparent ceramics. Dr. Yanagitani supported this author's view that S-FAP could not be made into a transparent laser quality ceramic. Non-cubic materials could not be made as laser quality transparent ceramics both because they are birefringent. Dr. Yanagitani suggested that the only way to make a ceramic non-cubic material truly transparent would be to put it in a very high magnetic field to align the grains.

Dr. Yanagitani also pointed out that while several groups have succeeded in making "transparent" YAG, their samples are not necessarily of laser quality. He mentioned that he had spent a few years developing transparent YAG and the next 10 years developing truly laser quality ceramics. He had been working on this development for the past ~15 years.

In addition to the YAG:Sm samples, Baikowski/Konoshima provided us with small circular samples, ~ 25 mm in diameter x 1-2 mm in thickness of YAG:Co<sup>3+</sup>; YAG:Cr<sup>4+</sup>, YAG:Yb<sup>3+</sup>, Y<sub>2</sub>O<sub>3</sub>:Yb<sup>3+</sup> and Lu<sub>2</sub>O<sub>3</sub>:Yb<sup>3+</sup>. Mr. Shigeta showed a slide with the space of stimulated emission cross section and lifetime that must be met by a ICF laser. While S-FAP is clearly within the allowable range of feasibility, the only ceramic to meet this criterion was cubic YAG:Yb, and YAG:Yb moves into the acceptable parameter area only at cryogenic (liquid nitrogen (LN)) temperatures (J. Dong, M. Bass, Y. Mao, P. Deng and F. Gan, J. Opt. Soc. Am. B, 20, 1975 (2003)). R. Beach pointed out that SrF<sub>2</sub>:Nd<sup>3+</sup> may also meet the criteria. However, Konoshima said the fluorides could not be fired in their furnace without fear of contamination. We are currently looking into the possibility of using YAG:Yb at temperatures near LN temperatures as an ICF laser gain media. Work has been started in this area in Japan and we will first assess the work in Japan and then simulate the overall laser energy balance, etc. A way to measure the low temperature spectra of the ceramic YAG:Yb has been identified.

## **Results/Technical Outcome**

We proposed that during this feasibility study and the first year of the LDRD, we would evaluate based on small samples whether or not ceramic YAG:Nd could be used in the SSHCL as the gain medium. At this time we are well ahead of that schedule. Konoshima has been able to provide us with the 10x10x0.6 cm sample mentioned above. They have also provided the actual size 10x10x2 cm slabs needed for installation in the SSHCL laser. These were procured under the SSHCL project budget. The critical optical properties been evaluated and four slabs have been received and cladded and are now available and ready to be installed in the laser test bed. The first very high powered (> 10 kW average power) laser using ceramic gain media will be ready for testing by mid February, 2005.

Our second objective was to make a small translucent piece of ceramic YAG in-house as part of the feasibility study and a semi- or transparent piece as part of the subsequent LDRD 05-ERD-037. We met this objective of the feasibility study and are progressing toward a transparent piece for the LDRD. Much of the work for the LDRD is on design of experiments (DoE's) aimed at not only producing a piece of

semi-transparent YAG but understanding what are the important process parameters in sintering ceramics to transparency.

Our third objective, namely, to obtain intellectual property on new ways to employ and take advantage of the properties of transparent ceramics in laser architectures is not as far along. As mentioned above IL-11317 has been filed and it provides protection for a much simpler and more advantageous means to suppress amplified spontaneous emission in a high-powered laser compared to diffusion bonding. If we had to have these ceramic slabs diffusion bonded or had to develop a co-sintering process as mentioned above, it would have resulted in a significant delay, at least three to six months.

#### **A) Evaluation of Konoshima/Baikowski ceramic YAG:Nd**

Our first samples of transparent ceramic YAG:Nd were two small samples obtained from VLOC Inc. in March, 2004. One contained 1 at % Nd and the other 4 at % Nd. Absorption and emission spectra were measured and were identical to those previously reported (Shoji, I, *et. al.* Appl. Phys. Lett. 77 #2, 939 (2000). X-ray diffraction showed a pattern similar to that of YAG powder indicating no crystal orientation. Scanning electron micrographs at LLNL did not show the grain structure seen in Figure 1 and it was felt that it would be necessary either to look very carefully with an optical microscope or to etch the surface prior to the SEM to see the grain structure. While doing this we were asked to return the samples to VLOC. EDAX showed no elements other than Al, Y and Nd. Since we were also asked not to modify the samples, no trace elemental analysis was performed. The samples were returned to VLOC in May.

The 10x10x0.6 cm sample was received in May, 2004. Gain measurements are shown in Figure 6. . The calculated curve was generated by Mark Rotter assuming a stimulated emission cross-section of  $2.8 \times 10^{-19} \text{ cm}^2$ , the value for crystalline YAG. A fit to the decaying portion of the curve yields a fluorescence lifetime of 235  $\mu\text{s}$ , in excellent agreement with the crystalline value (for this doping concentration) of 242  $\mu\text{s}$ .

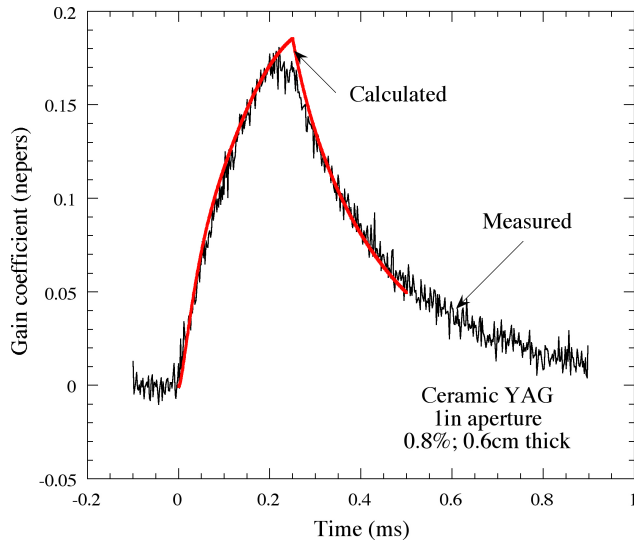


Figure 6. Measured and calculated gain coefficient for 10x10x0.6 cm ceramic YAG slab

In these experiments the diode pump light spectrum was adjusted by changing the temperature of the coolant water in order to optimize overlap with YAG:Nd absorption spectrum. Approximately 85 % of the diode light was absorbed. This sample was requested to have 0.8 at % Nd which was needed to insure absorption of the diode light in this thickness of sample. However, in order not to have parasitic lasing at this relatively high Nd concentration, it was necessary to reduce the aperture to  $\sim 1$  inch.

Scattering losses were also measured on this sample at Barr Assoc. in Massachusetts using a ring down lossmeter. The total loss measured was 190 to 220 ppm at 1064 nm. Of the average 205 ppm, about 35 ppm is surface scatter from the 3.5 to 4 Å rms surface roughness. The rest, 170 ppm, is bulk loss, absorption or scatter. The graph in Figure 7 shows how scattering losses in ceramic YAG have decreased in recent years to where they are equal to or below those found in single crystals.

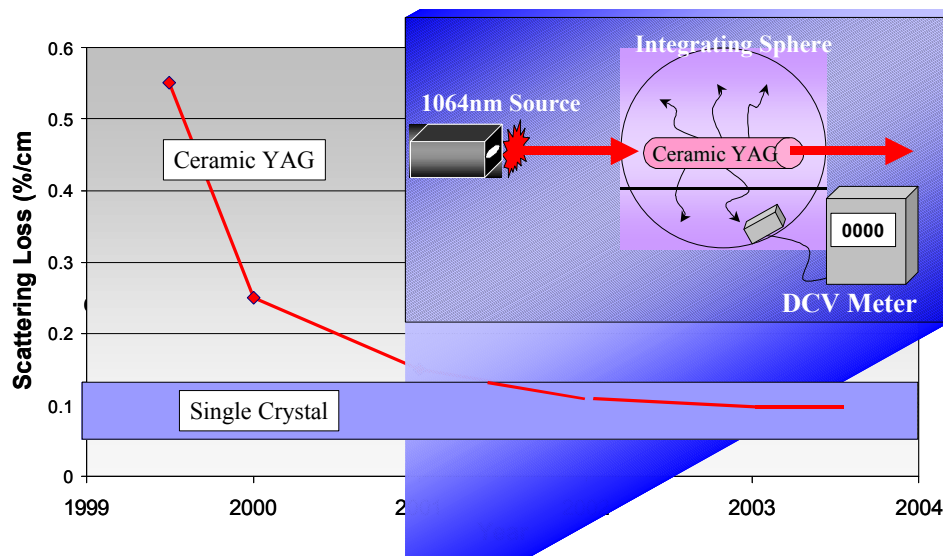


Figure 7. Measured scattering losses from transparent ceramic YAG samples over the past few years. Slide is from Baikowski International.

Figure 8 shows the gain measurements made on the 10x10x2 cm transparent YAG:Nd slabs shown in Figure 3 which were received in mid December, 2004. The first slab was epoxied into the blackened copper holder as shown in the left side of Figure 3. A second slab was supplied to us as defective, free of charge, since it had ~ 10 small inclusions or scattering sites. Our specifications had called for no inclusions. Nevertheless this slab was epoxied in a small blackened copper frame, 12 cm on a side with a thickness of 8 mm. This frame fits the present holders on the SSHCL laser. The slabs holder and the framed slab were individually placed in position in the SSHCL and were illuminated by the laser diode arrays of the laser. A small signal from a YAG:Nd probe laser was expanded to fill the aperture and amplified as it went through the slab.

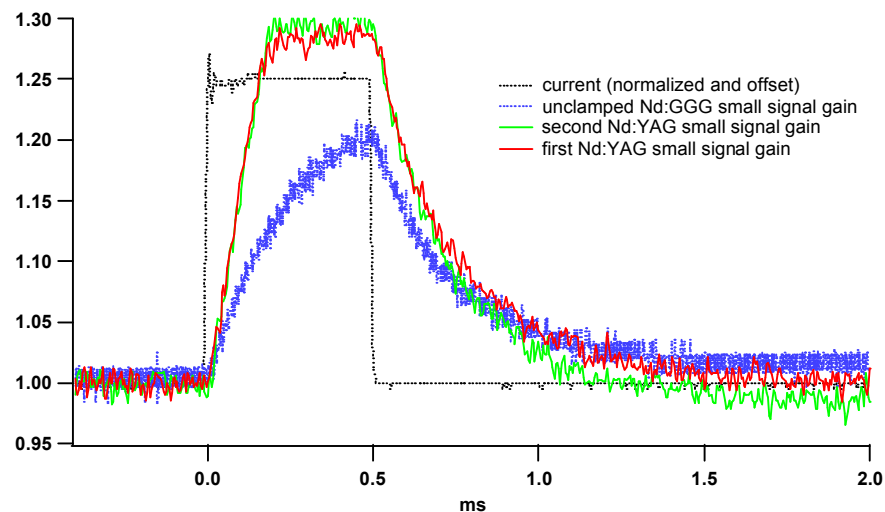


Figure 8. Gain measurements made on the first and second 10x10x2 cm transparent YAG:Nd slabs from Konoshima. The slabs were epoxy potted into blackened copper frames and placed in the SSHCL and pumped with the diode laser arrays of the laser. Also shown is the profile of the diode laser current and the the gain profile using a diffusion bonded GGG:Nd slab with the same diode array illumination.

The gain measurement profiles are similar for both the first and second slabs although the copper edge cladding holder geometries were different. The measurements show that parasitic lasing and clamping does occur with our method of ASE suppression. However, clamping does not occur until approximately 180 msec after the diode pump lasers are activated. At that point significant gain has been achieved. In the SSHCL operation, the SSHCL lases before this clamping occurs so it will not affect the performance. The diode laser pump light current profile is also shown. Also shown is the gain achieved with GGG:Nd slabs with GGG:Co diffusion bonded edge cladding. The maximum gain with GGG:Nd is ~ 1.19 while the ceramic YAG:Nd slabs yield a maximum gain of ~ 1.28.

Other specs were provided to Baikowski/Konoshima to insure a good wavefront and dimensional control. For example peak-to-valley rms surface distortion at  $0.6328 \mu\text{m} < 1/6 \lambda$ , gradient  $< 1/30 \lambda / \text{cm}$ , scratch/dig better than 5/10 were specified. The four slabs received so far have met or exceeded our specs with the exception that the second slab had a number of defect inclusions which were mapped x 35. Also all four slabs were intentionally sized toward the high end of our width spec  $100.5 \pm 0.5 \text{ mm}$ . The slabs were received with measured values for our specified parameters and we were provided with surface profiles measured with an interferometer.

We made additional measurements at the LLNL NIF large optic metrology lab on the third YAG:Nd ceramic slab that was received in January, 2005. Figure 8 shows the wavefront distortion as measured in a double pass beam measurement with a helium neon laser with the empty cavity wavefront removed.

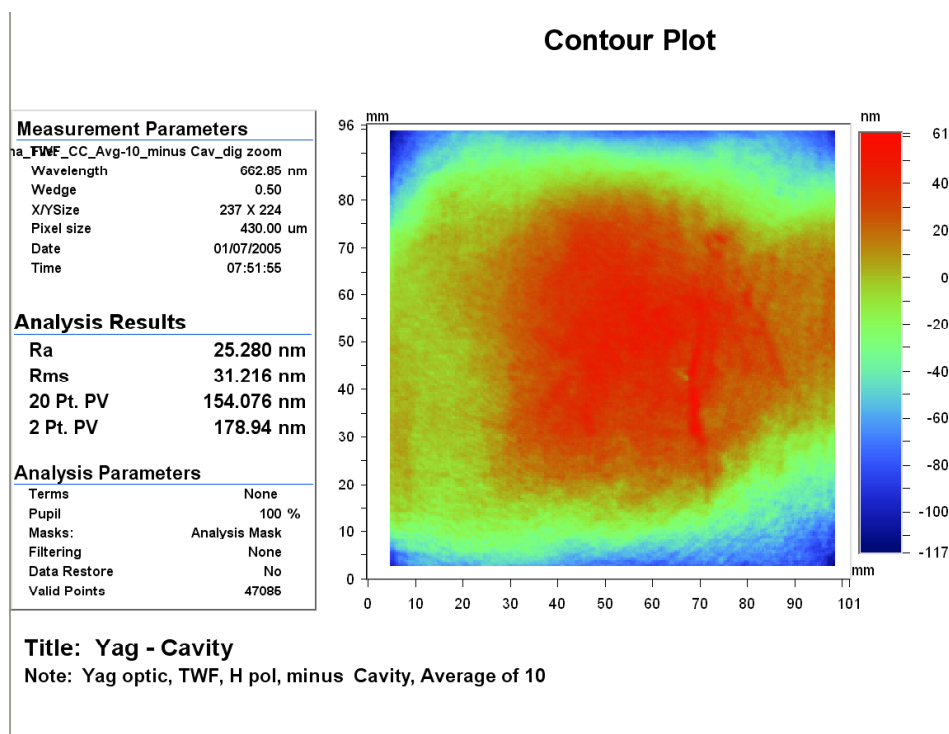


Figure 9. Contour plot of wavefront distortion of the third ceramic YAG:Nd 10x10x2 cm slab received from Baikowski/Konoshima. The plot is generated over the entire face of the slab in a double pass of the laser after subtracting the distortion due to the cavity without the slab.

Figure 9 shows that the rms wave distortion from a double pass is around 31 nm or  $\sim \lambda/21$ . The only distortion observed in this contour map occurs near the top and bottom edge and is not surprising given the nature of polishing.

Figure 10 and 11 shows a few of the results of small spot interferometry aimed at measuring surface roughness. Figure 9 shows micro-roughness measured over a very small spot. Three spots are shown: one near the center and two near edges. The average roughness depth is  $\sim 0.5 \text{ nm}$ . The only noticeable structural features are very small scratches near the center of the slab. These are polishing marks and are expected near the center. Figure 10 shows the results of PSD II, a filtered



roughness measurement, on larger spots. Rms values are  $\sim 1.5$  nm and again the only structures visible are polishing marks near the center of the slab.

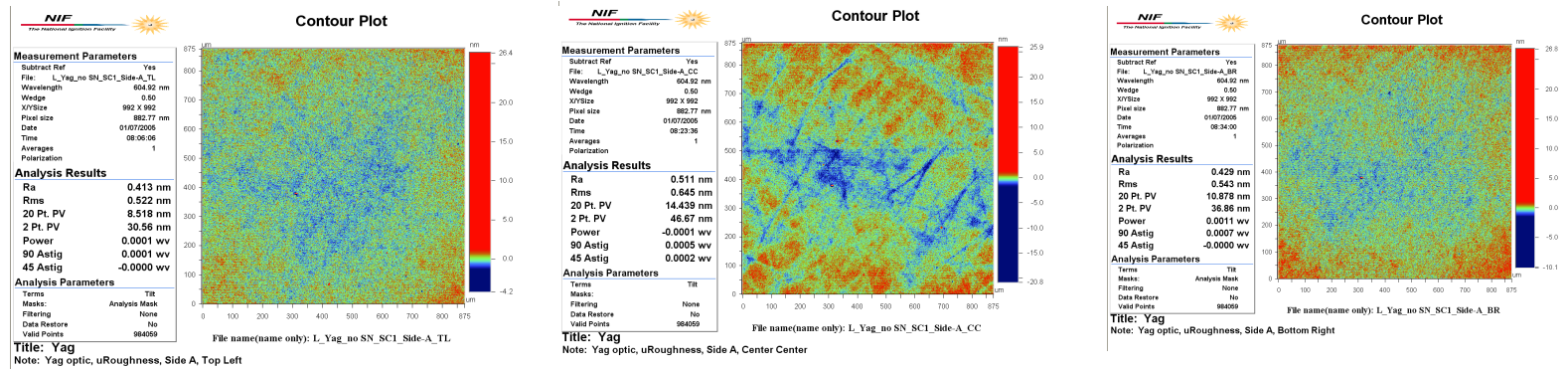


Figure 10. Contour plots of microroughness on three spots of the third YAG:Nd large slab from Baikowski/Konoshima as measured on small spots by interferometry. The slabs were polished at Baikowski, Japan. The figure on the left hand side is from from a spot in the upper left hand corner of the slab on side A. The figure in the center was obtained from an area in the center of the slab on the same side and the figure to the right was from near the lower right hand corner of the slab on side A.

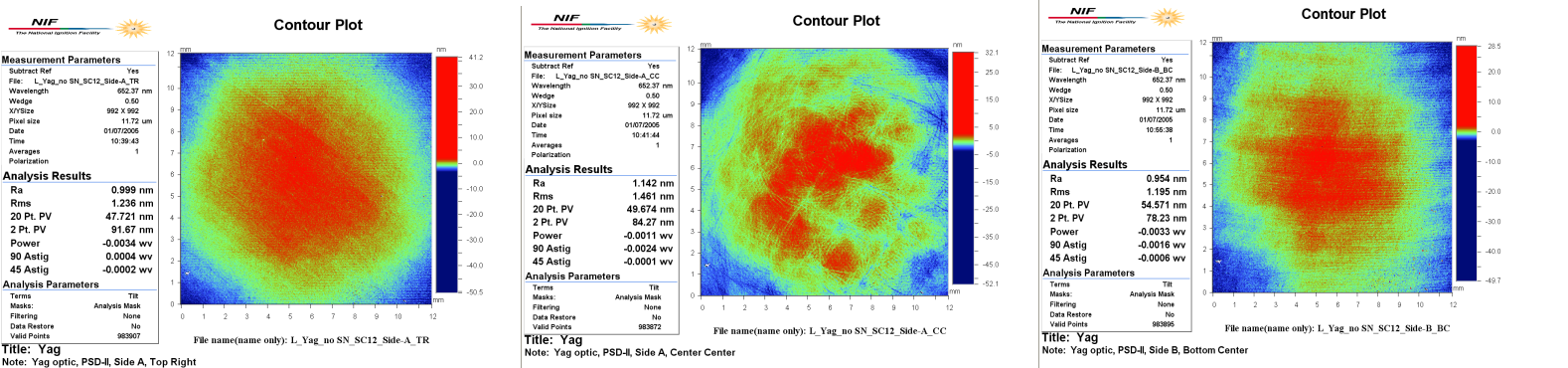


Figure 11. PSD II surface roughness measurements. The graph on the left hand side was taken from a spot near the upper left hand corner of side A of the third slab. The center contour is from the center of the slab and the figure on the right was from the upper right hand corner region. All are on the same side of the slab but are representative of both sides.

The slabs were also illuminated from the side with a long narrow side illumination lamp. Side illumination shows a inclusions, pores, etc. which scatter light. These will appear as bright specs against a dark background. Pictures taken with a high-resolution camera on the third slab with this illumination are shown in Figure 12. Other than a couple specs near the bottom of the photograph, there was no evidence of inclusions, pores or other scattering centers in this slab.

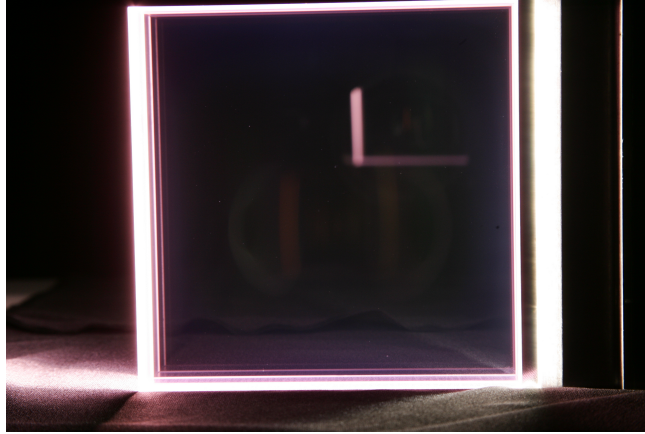


Figure 12. High resolution picture taken with Canon A10 digital SLR with 1 sec exposure of the third 10x10x2 ceramic YAG slab. The slab is illuminated with a linear lamp positioned along the center of the right hand edge of the slab. The vertical and horizontal white bars in the middle of the slab are reflections of the side light.

Similarly the front and back surfaces of the slab were side lit by moving the slab so that the lamp was in the plane of the surfaces. Surface scattering sites as well as any dust on the surface will be illuminated. Results are shown in Figure 12.

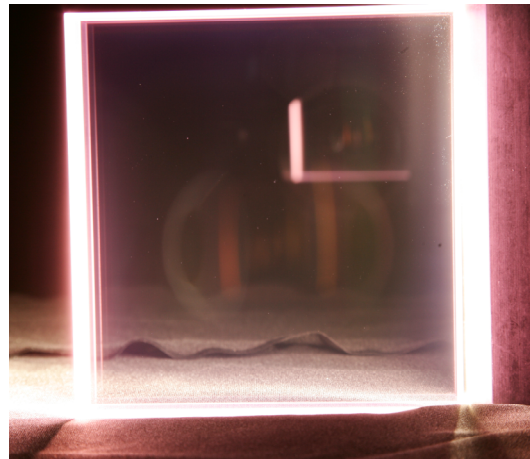
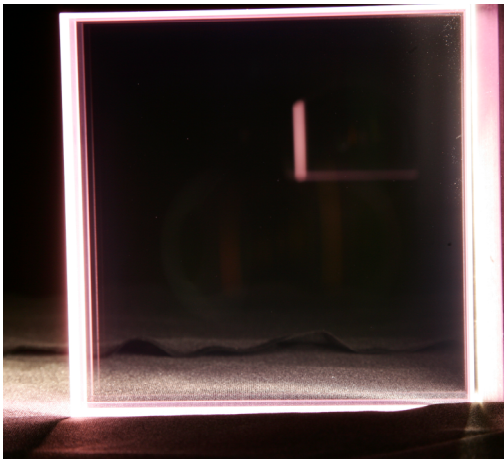


Figure 12. High-resolution 1 second exposure pictures of the third slab with front (left) and back (right) surfaces illuminated by linear side lamp along the right hand edge. Reflections of the side lamp can be seen as some small surface specs. Slab was drag wiped with alcohol dampened lint free cloth.

#### **B) Results of our in-house synthesis of transparent ceramic YAG**

As mentioned above our first sintering experiments were made using YAG powder commercially available from MTI corporation in Richmond, California. The powder

was pressed into pellets ~ 1 inch in diameter with and without binders and with and without silica to serve as a sintering aid. The pellets were sintered under vacuum at Thermal Technologies in Santa Rosa, California. The details of these experiments and the conditions of firing are described in the Interim Report. The Interim Report also shows pictures of the sintered samples and reports densities. The highest densities obtained were around 95 %. Some translucency not transparency was achieved.

A second set of experiments was performed at the University of California at Davis with Professor Zuhair Munir using his Spark Plasma Sintering (SPS) hot press. Again the MTI powder was used. The details of these experiments including the temperature of firing and the current profile are available from Professor Munir. Because the SPS uses a graphite anvil producing a reducing atmosphere, the samples turned dark gray to black. These samples were taken and re-fired in air at 1550 C overnight. This turned the samples white and we were able to shine light from an LED through the samples a couple of mm thick. One advantage of the SPS is that sintering can be carried out at lower temperatures thereby avoiding a lot of grain growth. Unfortunately we did not have the funds to support a post-doc to continue this work at UC Davis but we may be able to continue it in the coming year at least to determine whether this method could be used to improve transparency.

We also pursued more traditional methods of hot pressing and hot isostatic pressing at Greenleaf Corporation in Pennsylvania. Samples of the MTI powder were hot pressed at 1750C and 1800 C with 4.5 Kpsi pressure followed by two HIP'ings at 28.5 Kpsi at 1720 C. Again due to the graphite anvils used the samples were dark gray to black. They were then fired in air at 1550 C for 12 hours. The samples turned white but were still opaque. Densities after firing in air were ~ 95 % theoretical. Two more samples were sent to Greenleaf. One was a sample of Shin-

Etsu material and the other was a sample made by Brady Clapsaddle using the aerogel route described above. These samples were hot pressed at 1780 C and 4.5 Kpsi and subsequently HIP'ed at 1720 C and 28.5 Kpsi and measured 100 % density after sintering at Greenleaf. They have not yet been fired in air and are dull gray to black.

Brady Clapsaddle's aerogel powder (059\_B) was also vacuum fired at ~ 1750 at UC Davis in their vacuum Brew furnace. Samples pellets were prepared with and without 12 hour ball milling by dry pressing. Due to carbon in the furnace these samples were also gray after firing and were then refired in air at 1550 C. The resulting samples were translucent with some transparent regions and some evidence of abnormal grain growth. The areas of transparency were typically near edges of the pellets and could best be seen with a microscope at 5 times magnification as shown below.



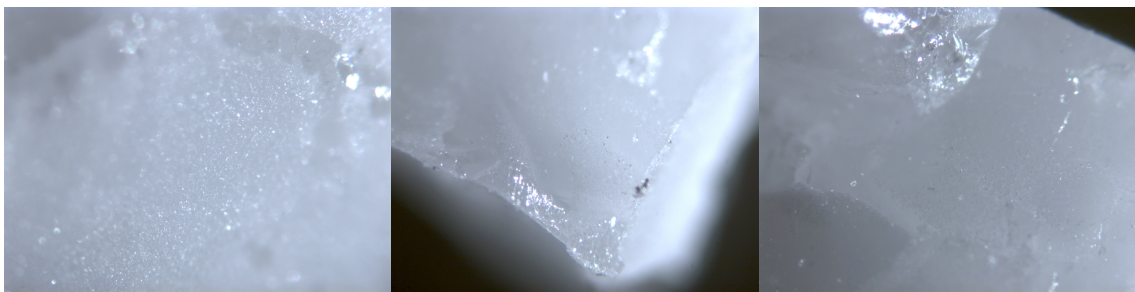


Figure 13. Microscope picture of regions of sample pellets made with aerogel powder dry pressed and vacuum sintered at  $\sim 1750$  C at UC Davis.

Our most recent samples have been vacuum fired in the furnace at Stanford University. We brought Shin-Etsu powder and powder from Brady's aerogel synthesis for firing there. Both powders were separated into two lots, one ball milled for 12 hours and the other not. Pressed pellets were made following the procedure mentioned above and the first firings had a high temperature soak for 3 hours. The pyrometer read  $\sim 1700$  C but it was felt that the temperature was actually higher than this. Pictures of the resulting samples are shown in Figure 14.

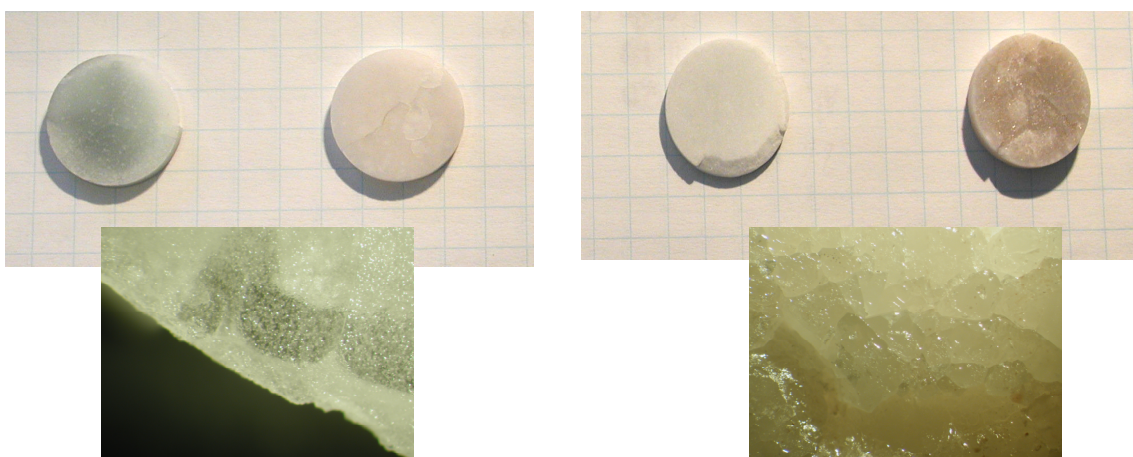


Figure 14. Pictures of the first pellets fired at Stanford in vacuum at  $\sim 1700$ C for 3 hours. The pellets on the left had side were made using the Shin-Etsu powder (Lot # RYAG-OCX-074) with (left) and without (right) ball milling for 12 hours. The samples on the right are from aerogel powders (BCVII082A). The pictures below are under 5x magnification (not ball milled samples).

Again these samples show regions of transparency and some abnormal grain growth. Unfortunately there was some nickel contamination from tantalum holders in the furnace resulting in the observed discoloration of the samples.

In order more systematically study the synthesis of transparent YAG and to go back to the process outlined in the Konoshima Japanese patent literature (T. Kokai Patent App. # HEI 10[1998]-101333), namely, co-precipitating YAG using ammonium hydrogen carbonate as illustrated below.

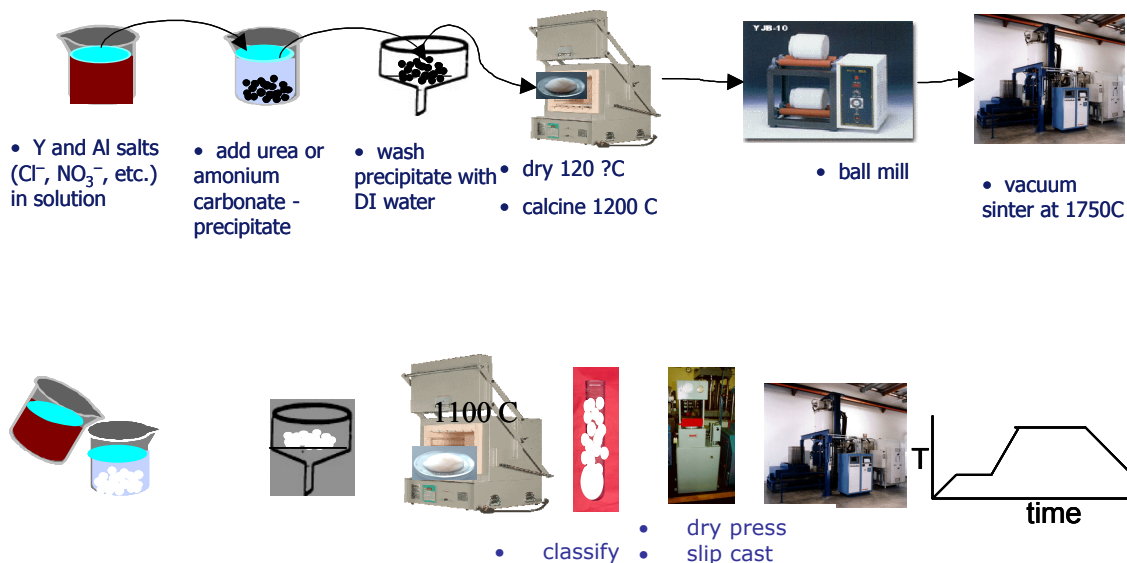


Figure 15. Top - schematic of the process outlined in the Japanese patents and literature referenced in the text. Bottom - schematic of process used at LLNL with added classifying step.

Since there are many process steps, we first prioritized by most likely to impact the critical properties of transparency and grain structure. Parameters in these steps still a fairly large number of parameters to be varied. Hence a two-level Plackett-Burnham design-of experiment (DoE) was constructed for the purpose of minimizing the number of experiments. Since this is a very sparse matrix, we hoped to learn only what the key variables were which determine transparency and grain structure. Subsequent DoE's would be used to optimize the process.

Two Plackett-Burnham DoE's were constructed: one for using the Shin-Etsu YAG powder and one including factors involved in precipitating our own starting powder.

The Shin-Etsu powder was cold pressed samples are prepared by mixing the raw powder (4g per pellet) with an organic binder (100mg PEG in EtOH / pellet). After drying, this mixture is uniaxially pressed in a stainless steel die at a pressure of 15000 psi. Vaseline is used to lubricate the die. The organic binder is burned out in air at 750°C for 4 hours.

Pellets were also made after first classifying the powder and by slip casting. The procedure for slip casting was developed by Richard Landingham:

### **Non-classified slip casting**

1. A Plaster Paris mold is prepared by mixing 60 gms of Plaster Paris (PP) powder with 30 ml of water. This mixture is poured into a box (1 1/2" by 2 1/2" by 4") and allowed to setup after pushing a 1" dia. steel rod into the smooth PP surface to a depth of 1". After the PP sets up, the steel rod is removed to form a 1" dia. cavity in the PP. The PP mold is then oven dried overnight at 60 C in air.
2. YAG powder (4.2 gms) is dispersed in a plastic container with 5 ml of demonized water (water contains a dispersing agent-0.0007 gm/ml of Dispex A40).
3. The YAG slurry is poured into the cavity of the PP mold after wetting the PP mold by pre-filling the cavity with water and allowing it to seep into the PP.
4. The water in the YAG slurry is allowed to seep into the PP while the YAG powder collects and shrinks at the bottom of the cavity.
5. The shrinkage causes a gap to form around the edges of the slip cast YAG powder. Once this gap forms, the mold and casting are dried in the oven at 60 C overnight.
6. The dry slip cast YAG pellet is removed from the cavity and measured and weighed to determine its density.
7. This YAG pellet is now ready for sintering.

#### **Classified slip casting**

1. Same procedure as 1. above.
2. Same procedure as 1. above except 35ml of water is mixed with the YAG powder.
3. The thin YAG slurry is dispersed with an ultrasonic probe (50% power and 3 sec. pulse rate) to break up soft agglomerates.
4. This dispersed slurry is allowed to settle for 5 min. before decanting off the top 30 ml of slurry. The remaining slurry contains the coarser particles and is dried and weighed.
5. The decanted 30 ml is allowed to settle for 15 hours and then 25 mls of water are decanted off the top of this slurry. The decanted water is dried and weighed for YAG fines lost to the slip casting.
6. The 5mls of slurry left after the second decant has the bulk of the finely dispersed YAG powder and is ready to be slip cast into the PP mold.
7. The YAG slurry is poured into the cavity of the PP mold after wetting the PP mold by pre-filling the cavity with water and allowing it to seep into the PP.
8. The water in the YAG slurry is allowed to seep into the PP while the YAG powder collects and shrinks at the bottom of the cavity.
9. The shrinkage causes a gap to form around the edges of the slip cast YAG powder. Once this gap forms, the mold and casting are dried in the oven at 60 C overnight.
10. The dry slip cast YAG pellet is removed from the cavity and measured and weighed to determine its density.

This YAG pellet is now ready for sintering.

The Plackett-Burham DoE is shown below along with a schematic of the temperature profile used in the Stanford firings.

Standard Order	Run Order	Classify yes = 1 no = -1	Pill CIP = 1 Slip cast = -1	$h_R$ 600 C/h = 1 300 C/h = -1	$T_s$ 1730 C = 1 1780 C = -1	$t_s$ 3 hours = 1 72 hours = -1
7	1	-1	1	1	1	-1
8	2	-1	-1	1	1	1
9	3	-1	-1	-1	1	1
2	4	1	1	-1	1	-1
4	5	1	-1	1	1	-1
6	6	1	1	1	-1	1
10	7	1	-1	-1	-1	1
5	8	1	1	-1	1	1
12	9	-1	-1	-1	-1	-1
1	10	1	-1	1	-1	-1
11	11	-1	1	-1	-1	-1
3	12	-1	1	1	-1	1

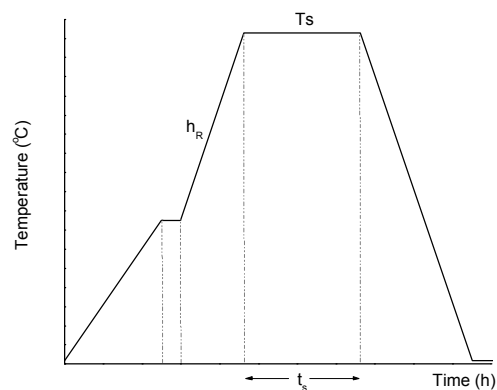


Figure 16. Plackett-Burnham DoE for firing Shin-Etsu YAG powder. On the right side is a schematic of the temperature profile used.

The second DoE involved all the critical or key process steps identified including the precipitation of the raw material powder as well as the firing.

Standard Order	Run Order	Al(NO <sub>3</sub> ) <sub>3</sub> = 1 Alum = -1	Carbonate Conc High = 1 Low = -1	Dispersant with = 1 without = -1	Temperature >90C = 1 RT = -1	Stirring speed Fast = 1 Slow = -1	Age hot for 2 days yes = 1 no = -1	Wash with HNO <sub>3</sub> yes = 1 no = -1	Classify yes = 1 no = -1	Pill Cold press = 1 Slip cast = -1	Ramp rate fast = 1 slow = -1	Temperature 1700 C = 1 1780 C = -1	Dwell time 3 hours = 1 3 days = -1	Response Transmission	Response Density	Response Ave. grain size
19	1	-1	1	1	-1	-1	-1	-1	-1	-1	1	-1	1			
14	2	-1	-1	1	-1	-1	1	-1	-1	1	1	-1	-1			
8	3	1	1	1	1	-1	1	-1	-1	-1	1	1	-1			
1	4	1	-1	1	1	-1	-1	-1	-1	1	-1	1	-1			
17	5	1	-1	-1	-1	-1	-1	1	1	-1	1	1	1			
3	6	-1	1	1	-1	1	-1	1	1	-1	-1	1	-1			
12	7	1	-1	1	-1	1	1	1	1	-1	-1	1	1			
18	8	1	1	-1	-1	-1	1	-1	-1	1	-1	1	1			
6	9	1	1	-1	-1	1	-1	1	1	1	-1	-1	-1			
5	10	1	-1	-1	1	1	1	-1	1	-1	-1	-1	-1			
15	11	-1	-1	-1	1	-1	-1	1	1	1	1	1	-1			
10	12	1	-1	1	1	1	-1	1	1	-1	1	-1	1			
4	13	-1	-1	1	1	-1	1	1	1	-1	-1	-1	1			
20	14	-1	-1	-1	-1	-1	-1	-1	-1	-1	-1	-1	-1			
7	15	1	1	1	-1	-1	1	1	-1	1	1	-1	-1			
16	16	-1	-1	-1	-1	1	1	-1	-1	1	1	1	1			
2	17	1	1	-1	1	1	-1	-1	-1	-1	1	-1	1			
11	18	-1	1	-1	1	1	1	1	-1	-1	1	1	-1			
9	19	-1	1	1	1	1	-1	-1	1	1	-1	1	1			
13	20	-1	1	-1	1	-1	1	1	1	1	-1	-1	1			

Figure 17. Plackett-Burnham DoE for LLNL procedure for precipitating YAG powder and sintering.

All solutions were made using distilled, deionized water (d<sup>2</sup>-H<sub>2</sub>O) with an initial resistivity of 18 MΩ. Alum (AlNH<sub>4</sub>(SO<sub>4</sub>)<sub>2</sub>·12H<sub>2</sub>O; Fluka, ≥ 99.0%), aluminum nitrate nonahydrate (Al(NO<sub>3</sub>)<sub>3</sub>·9H<sub>2</sub>O; Alfa Aesar, 98.0 – 102.0%), yttria (Y<sub>2</sub>O<sub>3</sub>; Alfa Aesar, 99.999%), and ammonium bicarbonate (NH<sub>4</sub>HCO<sub>3</sub>; Alfa Aesar, 99%) were all used as

received. Nitric acid ( $\text{HNO}_3$ ; J. T. Baker, 69.0 – 70.0%) was diluted with water in a 1:5 (v:v) ratio. Two separate 15 L solutions of 0.15 M  $\text{Al}^{3+}$ /0.090 M  $\text{Y}^{3+}$  were prepared with yttria (151.29 g, 0.67 mols) and either alum (1020.00g, 2.25 mols) or aluminum nitrate nonahydrate (844.05 g, 2.25 mols) to obtain stock solutions containing  $\text{Al}^{3+}$  and  $\text{Y}^{3+}$  in a Al:Y molar ratio of 5:3. The stock solutions were prepared by first slurring the yttria and aluminum salt in 2.25 L of  $\text{d}_2\text{-H}_2\text{O}$  followed by addition of 0.6 L of the diluted nitric acid solution. This mixture was then gently heated to  $\sim 80^\circ\text{C}$  until all solids were observed to be dissolved. After the mixture cooled to room temperature, the resulting solution was diluted to a final volume of 15 L. Ammonium bicarbonate (2371.80 g; 30 mol) solutions were made at a concentration of 1.5 M in 20 L batches by dissolving the salt in  $\text{d}_2\text{-H}_2\text{O}$ . All stock solutions were stored at room temperature in 20 L, HDPE carboys prior to use. For precipitation experiments, 1200 mL of stock metal salt solution\* (0.15 M  $\text{Al}^{3+}$ /0.090 M  $\text{Y}^{3+}$ ) was added drop wise to 1800 mL of stock  $\text{NH}_4\text{HCO}_3$  (1.5 M)\* containing a dispersant\* (0 or XXX mL Dispex<sup>TM</sup>). During addition, the mixture was stirred\* (vigorous or gentle agitation) at the desired temperature\* (R.T. or  $90^\circ\text{C}$ ). Following precipitation, the precipitate was aged\* (0 or 2 days) at room temperature without stirring. The aged precipitate was then vacuum filtered, washed 4 times with  $\text{d}_2\text{-H}_2\text{O}$ , rinsed with ethanol, and dried at room temperature under flowing nitrogen. The resulting cake was then ground with a mortar and pestle. The ground powder was then calcined in air at  $1100^\circ\text{C}$  for 1 hour with a heating rate of  $2.5^\circ\text{C}/\text{min}$ . Following calcination, some batches of powder were washed\* with 2 M  $\text{HNO}_3$ , followed by 4 washings with  $\text{d}_2\text{-H}_2\text{O}$ . Washed powders were dried at  $80^\circ\text{C}$  overnight.

Further details on these DoE's as well as the response values including measures of transparency and grain structure and the results of the DoE analysis will be reported in the 2005 LDRD final report.

## **C) Novel Laser Architectures using Ceramics and Other Applications**

### **1) Integral Edge Cladding with YAG:Sm<sup>3+</sup>**

As mentioned above we discussed the possibility of co-sintering an edge-cladding onto the amplifier slab so that ASE suppression would be obtained in a single monolithic piece. YAG:Sm<sup>3+</sup> would have the advantage of not absorbing the diode pump light. This would make it possible to either face or edge pump the slabs through the edge cladding. Konoshima offered that it was developing the technique whereby it would sinter both the slab and edge cladding near the final result and then complete the sintering with the pieces attached. They will then diffuse into each other with diffusion distances of 30 or so microns. This diffusion is considerable more than would occur if single crystals were polished and diffusion bonded.

In order to determine if YAG:Sm<sup>3+</sup> would work for the edge cladding we obtained samples of transparent YAG with 3 at % Sm 0.135 cm thick and  $\sim 2$  cm in diam; 5 at % Sm 0.158 cm thick and 5 at % 0.594 cm thick. Another thick sample showed evidence of scattering and was not used. The figures below show spectra obtained on these samples.



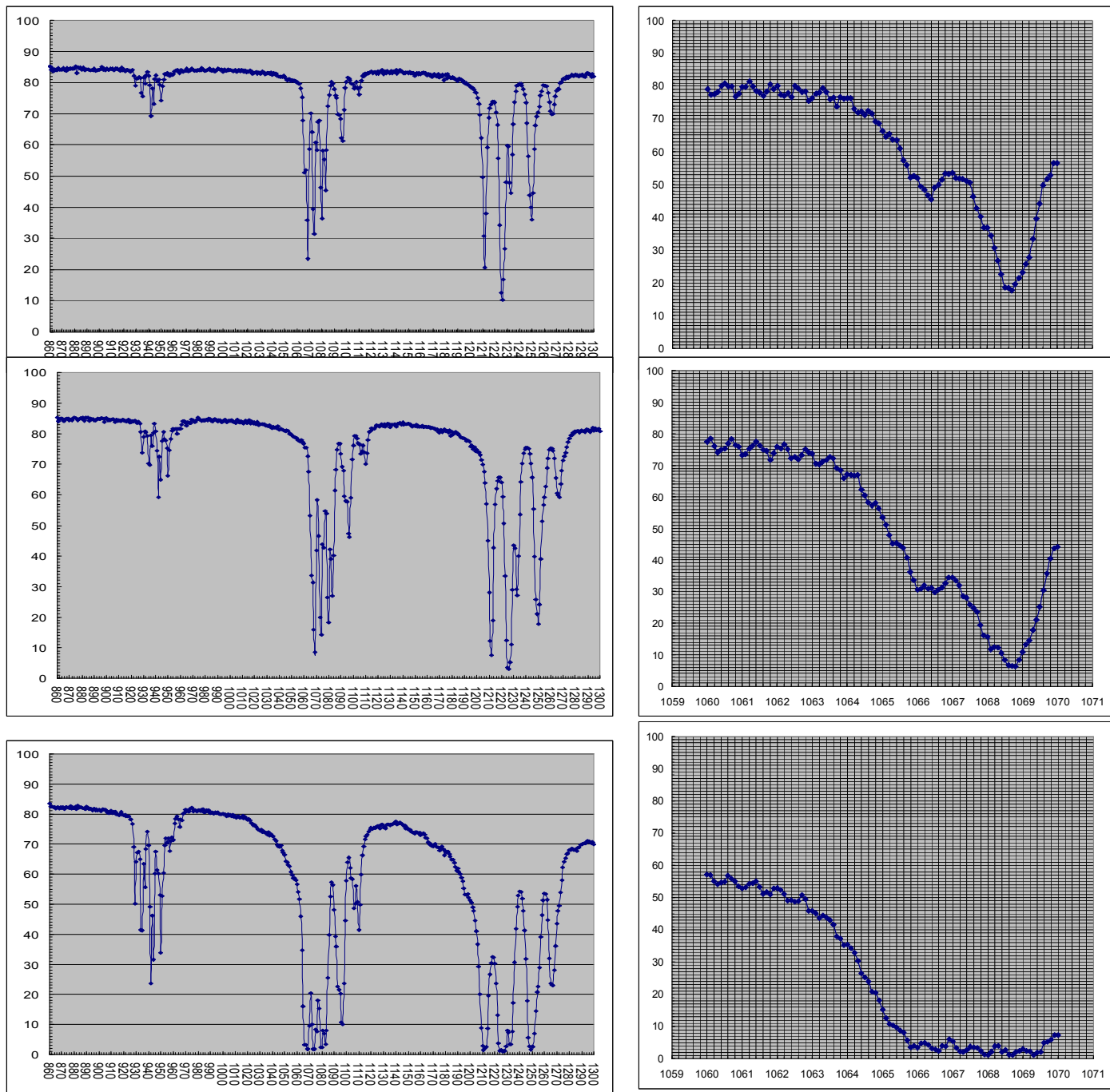


Figure 18. Top. Spectra of ceramic YAG: 3 at % Sm, thickness = 0.135 cm. Right hand side shows a blowup of the wavelength range from 1060 to 1070 nm. Middle. Spectra of YAG:5 at % Sm, thickness = 0.158 cm. Bottom. Thick, 0.594 cm sample with 5 at % Sm.

From the high resolution spectra we obtained the following absorption coefficients at 1064.2 nm: 0.194 (1/% cm) from 3 at %, 0.156 from 5 at %, 0.168 from the thick sample and 0.134, 0.149 and 0.143 (1/ % cm) at 1064.0 nm. There is some

uncertainty due to the determination of the baseline. Nevertheless at 5 at % absorption coefficients of 1.0 or 0.7 (1/cm) will be sufficient to absorb the ASE with 1 cm thick edge cladding. 0.6 (1/cm) is the value currently targeted for the GGG cladding. We will be pursuing the YAG:Sm integral edge cladding during the 2005 LDRD.

## **2) Ceramic laser materials for the Mercury Laser**

Several other transparent ceramic material samples were obtained from Konoshima/Baikowski for evaluation for the Mercury Laser. These included  $\text{Y}_2\text{O}_3$ : 10at%  $\text{Yb}^{3+}$ ;  $\text{Lu}_2\text{O}_3$ : 3at%  $\text{Yb}^{3+}$  and YAG: 9.8at%  $\text{Yb}^{3+}$ . Yb has the advantage of a longer lifetime than Nd and hence requires less pump light for inversion. Discussions with Ray Beach and Steve Payne on other requirements of the Mercury ICF laser eliminated yttrium oxide and lutecium oxide and most other cubic oxides from consideration. As mentioned above the Japanese are pursuing YAG:Yb at liquid nitrogen temperatures. Ray Beach has been evaluating the parameters and we are pursuing measurements that may be needed to appropriately evaluate this alternative. Also suggested is ceramic  $\text{SrF}_2$ :Nd that similarly has a very long lifetime. So far we have not identified a possible source for firing this material. Precipitating Sr or Ca fluoride is in fact an easily implemented process since both fluorides are very insoluble and can be precipitated from a water solution of the metal salts with a solution of ammonium hydrogen fluoride.

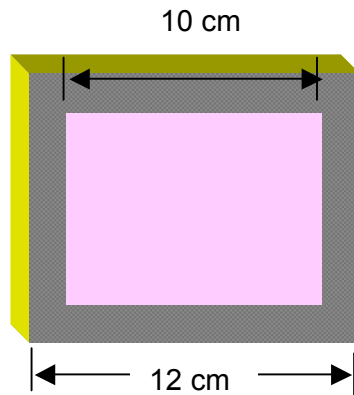
## **3) Applications for Transparent Ceramics in NIF**

NIF requires very large optics 30-40 cm on a side. There are currently no commercially available vacuum furnaces for firing such large ceramics. However, we are looking to identify any custom built furnaces that might serve this purpose. It is doubtful that NIF would be interested in trying to fabricate transparent ceramics for any application where they can currently use glass or fused silica optics. However, in areas where any material being used damages from  $3\omega$  radiation and there are no other options ceramics might be considered. The first question is whether ceramic YAG or other ceramic material (Steve Payne has suggested  $\text{CaF}_2$  because of its large band gap) would be much less apt to damage than current single crystals, glass or fused silica. Pam Whitman has suggested that surface damage growth might be impeded by the grain boundaries. During the next few months we plan to obtain undoped YAG and do damage testing which LLNL is well equipped to do in order to answer these questions.

## **4) Novel Laser Architectures**

The pictures below show several novel laser amplifier architectures including the integral edge cladding and amplifier; a composite amplifier wherein the Nd doped YAG is embedded in undoped YAG designed to serve as a light pipe for the diode pumping to allow for both edge and face pumping, and a passive Q-switched laser with the saturable absorber  $\text{YAG:Cr}^{4+}$  dispersed throughout rather than as a separate optical element. These and other ideas will be evaluated as to their utility and feasibility in coming months. Disclosures will be written on those that warrant further study. Some of the physicists in NIF may offer still other ideas as this material opens up the design space to different laser improvements.

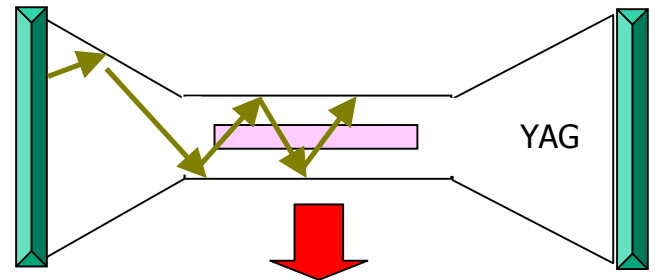
1)



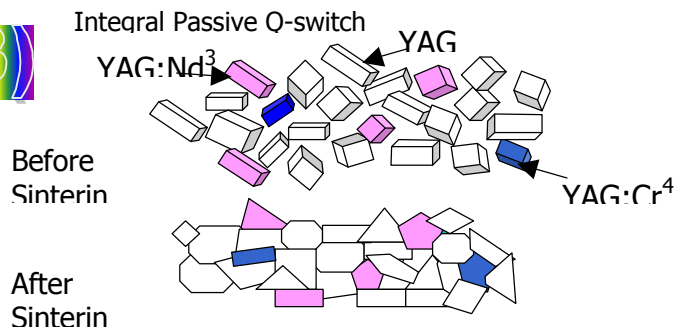
$$\alpha = 0.2 (\% \text{ Sm cm})^{-1} \text{ at } 1064 \text{ nm}$$

2)

### Enhanced Edge Light Pumping in Small Space



3)



	Separate (conventional) Q-switch	Comingled powder: YAG:Nd <sup>3+</sup> + YAG:Cr <sup>4+</sup> + YAG
Stored energy prior to Q- switching	0.74 J	3.89 J
1064 nm gain after Q-switch	1.4 nepers	7.4 nepers
Output pulse energy	0.24 J	1.15 J
Q-switched pulse width	8.5 nsec	1.4 nsec

Figure 19. Some novel integral multifunctional laser architectures using sintered ceramics: 1) YAG:Sm ASE suppressor sintered directly to the YAG:Nd amplifier slab in one piece. 2) An optical wave guide or non-imaging collector for focusing diode light on both edges and faces of the Nd doped region of a monolithic composite YAG and YAG:Nd structure. 3) YAG:Cr a saturable ASE absorber comingled with YAG and YAG:Nd to produce a more powerful passive Q-switched laser.

## **Exit Plan**

Following the feasibility study **UCRL-04-FS-006** we proposed an LDRD project which was approved as **05-ERD-037** for **\$150K**. The LDRD was proposed as a three year project. The 2005 deliverables were: determination of the feasibility of using ceramic YAG:Nd in the SSCL laser, a small piece of transparent or nearly transparent ceramic YAG made in-house and IP on novel applications for ceramic materials in high powered lasers. Objectives for the out years included fabricating or procuring large transparent optical components for LLNL lasers, gaining an understanding of what are the important parameters needed to synthesize transparent ceramics and determining the feasibility of making other optical materials as ceramics.

We are aware the DARPA has a solicitation in this area and we will pursue this as soon as the solicitation is made available.

As we go forward and demonstrate the utility of ceramics for LLNL high powered lasers, we expect that ceramic laser parts will become part of these laser plans and therefore will be funded by the agencies supporting the lasers and the projects themselves.

The close working relationships that we have established with Konoshima/Baikowski and Stanford University may also lead to joint funding in the future.

## **Summary**

We have evaluated ceramic YAG:Nd for use in high-powered lasers, in particular, the SSHCL laser and have certified it as a replacement for the current single crystal GGG:Nd. We have designed and procured 10x10x2 cm YAG:Nd amplifier slabs for the SSHCL and developed a means for edge-cladding these amplifiers to suppress ASE. These will be installed in the SSHCL shortly. This laser will be the first high powered laser to use ceramic gain media.

We have also begun a program to make in-house transparent ceramic YAG. The development of the process for making transparent ceramic YAG in Japan took approximately 15 years of focused effort and so it is not surprising that we do not have samples of laser quality at this time. Nevertheless we have made several translucent pieces and a few with transparent regions in the sintered pellets. We have also designed a large DoE to determine the key factors or parameters in the process.

Several other applications of transparent ceramics in high-powered lasers of interest to NIF are being investigated. These include the use of ceramic materials in the Mercury laser and possible use of ceramic filters or optics in NIF when no other solution is available. A number of novel laser architectures enabled by transparent ceramics are also being looked at including: incorporation of edge cladding into the amplifier piece, monolithic structures including light guides for optical pumping of the gain region, meso-scopic structure ceramics including commingling of YAG:Cr as a saturable ASE absorber, and others.

**Acknowledgements (if applicable)**

We wish to acknowledge the the help of the SSHCL team including Robert Yamamoto, Scott Fochs, Mark Rotter, Charles Parks and Balbir Bhachu for their work and support of this effort and making the evaluation of ceramic YAG:Nd for the SSHCL possible. We appreciate the co-operation with Baikowski/Konoshima in providing transparent ceramic slabs of high quality, on time and to our custom specifications. We would like to thank Steve Letts for his help in developing the method of edge cladding. Ray Beach and Steve Payne offered interest and insights into ceramics for other applications. Romain Gaume, Jeff Wisdom and Professor Robert Byer of Stanford have been very cooperative in working with us in developing a joint route to transparent YAG. Finally we would like to thank Professor Zuhair Munir for letting us sinter some of the YAG powders in his Spark Plasma Sintering hot press.

**References**

Provided in the text.